

Efficient Event-based Semantic Segmentation with Spike-driven Lightweight Transformer-based Networks

Xiaxin Zhu¹, Fangming Guo¹, Xianlei Long^{*1}, Qingyi Gu², Chao Chen¹, and Fuqiang Gu¹

Abstract—Event-based semantic segmentation has great potential in autonomous driving and robotics due to the advantages of event cameras, such as high dynamic range, low latency, and low power cost. Unfortunately, current artificial neural network (ANN)-based segmentation methods suffer from high computational demands, the requirements for image frames, and massive energy consumption, limiting their efficiency and application on resource-constrained edge/mobile platforms. To address these problems, we introduce SLTNet, a spike-driven lightweight transformer-based network designed for event-based semantic segmentation. Specifically, SLTNet is built on efficient spike-driven convolution blocks (SCBs) to extract rich semantic features while reducing the model’s parameters. Then, to enhance the long-range contextual feature interaction, we propose novel spike-driven transformer blocks (STBs) with binary mask operations. Based on these basic blocks, SLTNet employs a high-efficiency single-branch architecture while maintaining the low energy consumption of the Spiking Neural Network (SNN). Finally, extensive experiments on DDD17 and DSEC-Semantic datasets demonstrate that SLTNet outperforms state-of-the-art (SOTA) SNN-based methods by at least 7.30% and 3.30% mIoU, respectively, with extremely 5.48× lower energy consumption and 1.14× faster inference speed.

I. INTRODUCTION

Semantic segmentation [1] aims to divide visual data into distinct regions with clear semantic properties, thereby enabling a deep understanding and analysis of the scene. This technology plays a crucial role in various cutting-edge fields such as autonomous driving, security monitoring [2], and robotics [3], forming the foundational component for environmental perception capabilities of intelligent robotics [4]. However, with the increasing accuracy and efficiency demands for robotics in high-dynamic, complex scenarios, traditional image-based semantic segmentation methods show significant performance degradation when processing high-dynamic or variable lighting scenes [3].

Event cameras, leveraging their innovative biomimetic event generation characteristics, have inspired considerable research interests in computer vision and robotics communities [5]. Event cameras [6] excel at detecting variations in light intensity at the pixel level with remarkable microsecond resolution. They asynchronously produce an event

stream that consists of time stamp t , spatial coordinates (x, y) , and polarity $(+, -)$. The event-driven nature of these cameras shows several superior advantages, including HDR perception, low latency, low energy cost, and enhanced sparsity, showing promising solutions to computationally intensive semantic segmentation. Although research on event-based semantic segmentation is still in its infancy, several works have been proposed. Ev-SegNet [7] develops the first baseline using solely events but requires a substantial computational load. Following this, DTL [8], Evdistill [9], and ESS [10] attempt to compensate for the lack of visual details in event data through transfer learning or knowledge distillation technologies from image processing branches. However, existing methods either are still computationally expensive or require auxiliary images. Therefore, a critical challenge is how to design an efficient and robust event-based segmentation model with lower computational and energy costs, sufficient event feature extraction ability, and without requirement for auxiliary modality.

With the development of biological computing, Spiking Neural Network (SNNs) is a potential solution inspired by mechanisms of information generation and transmission in the brain, which can convey dynamically generated binary spikes across spatial and temporal dimensions [11]. Thus, SNNs demonstrate excellent advantages in computation efficiency, temporal memory capacity, and biological interpretability. The basic building block of SNNs is the spiking neuron, which shares a highly similar generation mechanism with the event cameras, making SNNs theoretically well-suited to work with such cameras. Encouraged by these advantages, Kim et al. [12] attempt to integrate SNNs with classical ANN-based segmentation networks, but the performance is poor due to the plain feature extraction module. This indicates that combining the SNNs with event segmentation still requires further exploration.

To address the aforementioned issues, we propose SLTNet, a Spike-driven Lightweight Transformer-based semantic segmentation network that utilizes events only to achieve energy-efficient and robust performance. SLTNet is a hierarchical single-branch SNN-based method equipped with an encoder-decoder structure. It can extract both detail and semantic information while maintaining high efficiency and low energy consumption. Specifically, as shown in Fig. 3, SLTNet contains four stages in the encoder part, which includes three novel Spike-driven Convolution Blocks (SCBs) that capture fine-grained textural information, and two newly designed Spike-driven Transformer Blocks (STBs) that are responsible for extracting long-range contextual features in

*This work is supported by China Postdoctoral Science Foundation (No. 2023M740402), by National Natural Science Foundation of China (No. 42174050, No. 62403085), and Chong Startup Project for Doctorate Scholars (No. CSTB2022BSXM-JSX005). Corresponding: Xianlei Long.

¹X. Zhu, F. Guo, X. Long, C. Chen and F. GU are with the College of Computer Science, Chongqing University, Chongqing, China. (e-mail:202214021084t@stu.cqu.edu.cn; {202114131181, xianlei.long, cschaochen, gufq}@cqu.edu.cn)

²Qingyi Gu is with the Institute of Automation, Chinese Academy of Sciences, Beijing 100190, China (e-mail: qingyi.gu@ia.ac.cn).

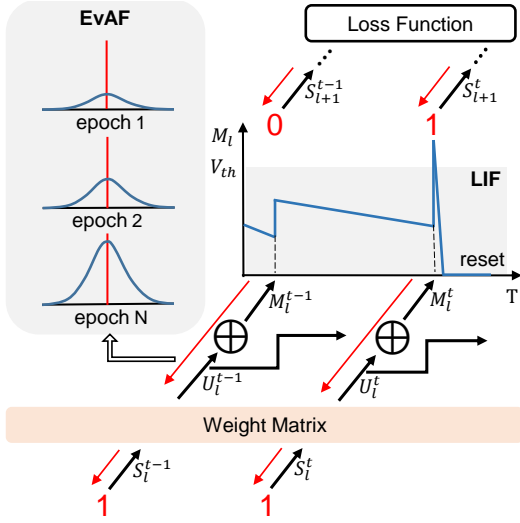


Fig. 1. The workflow of the evolutionary spiking neuron model in our algorithm. The black line denotes the forward propagation route, while the red line indicates the backward propagation process.

the last stage. Then, to further reduce the computational cost, we propose a Spiking Lightweight Dilated module (Spike-LD) that serves as the basic blocks of our conv-based SCBs and decoders. Finally, extensive experimental results conducted on two public event segmentation datasets demonstrate that the SLTNet outperforms competitive SOTA methods by at least 7.30% and 3.30% mIoU.

Main contributions of this work can be summarized as:

- We propose a novel Spike-driven Lightweight Transformer-based segmentation network (SLTNet) with events only to deal with high-dynamic complex scenarios, which is constructed on the basic SCBs and STBs that enable high-efficiency feature extraction and low computation cost.
- To reduce model parameters while maintaining efficient feature extraction ability, we design a Spiking Lightweight Dilated module, named Spike-LD, that can capture multi-scale event features concurrently and can easily adapt to SNN architectures.
- To enhance feature interaction capabilities, we propose novel Spike-driven Transformer Blocks, named STBs, by leveraging the re-parameterization convolution technique and spike-driven multi-head self-attention mechanism to achieve long-range contextual feature interaction with only floating-point accumulation operations.
- Extensive experimental results show that SLTNet outperforms SNN-based methods by at least 7.30% and 3.30% mIoU with much lower computation cost.

II. EFFICIENT BUILDING BLOCKS

A. Evolutionary Spiking Neuron Module

To construct a robust evolutionary spiking neuron (ESN) in SLTNet, we employ the Leaky Integrate-and-Fire (LIF) as the basic neuron due to its excellent biological interpretability and computational efficiency. We show its workflow

in Fig. 1. Mathematically, we explicitly formulate ESN's iterative forward propagation process as follows:

$$\begin{aligned} M_l^t &= \tau U_l^{t-1} + W_l^t X_{l-1}^t, \\ S_l^t &= H(M_l^t - U_{th}), \\ U_l^t &= U_{reset} S_l^t + U_l^t (1 - S_l^t), \end{aligned} \quad (1)$$

where the U_l^t is the membrane potential of neurons in the l^{th} layer at time step t , W_l^t is synaptic weight matrix between layers $l-1$ and l , S_l^t is the output of current layer, and τ is membrane time constant. The LIF module assumes that neurons accumulate membrane potential like a capacitor. They receive the leaky membrane potential of the previous time step τU_l^{t-1} and calculate current potential $W_l^t X_{l-1}^t$. When the accumulation reaches a certain threshold U_{th} , the neuron fires, generating a spike S_l^t using Heaviside step function $H(\cdot)$; otherwise, it remains zero. After firing, the membrane potential rebound to U_{reset} .

We train our model with an end-to-end strategy, so the back-propagation in ESN module can be described as:

$$\frac{\partial L}{\partial W^t} = \sum_i \left(\frac{\partial L}{\partial S^t} \frac{\partial S^t}{\partial U^t} + \frac{\partial L}{\partial U^{t+1}} \frac{\partial U^{t+1}}{\partial U^t} \right) \frac{\partial U^t}{\partial W^t}, \quad (2)$$

where L represents the loss function, W^t denotes the weights, and S^t and U^t indicate the activated spike and membrane potential, respectively.

The gradient of the spiking activity function S^t/U^t signifies their non-differentiable nature: either at a standstill or escalate to infinite magnitudes. We solve this problem by utilizing the evolutionary surrogate gradient function, called EvAF [13]. It will dynamically adapt to generate substitute gradient values as epochs iterate:

$$\begin{aligned} \varphi(x) &= \frac{1}{2} \tanh K(i)(x - U_{th}) + \frac{1}{2}, \\ K(i) &= \frac{(10^{\frac{i}{N}} - 1)K_{max} + (10 - 10^{\frac{i}{N}})K_{min}}{9}, \end{aligned} \quad (3)$$

where $i \in [0, N-1]$ is the index of training epoch. Following the common setup in [13], we set $K_{min} = 1$ and $K_{max} = 10$.

B. Spiking Lightweight Dilated Module

As illustrated in Fig. 2, the Spiking Lightweight Dilated (Spike-LD) module adopts a bottleneck structure [14] with a membrane shortcut. In this design, the module establishes a shortcut connection between the membrane potential of spiking neurons, addressing the vanishing gradient problem by achieving identity mapping in a spike-driven mode. Then, it integrates the spiking paradigm by following the weight computation stage with batch normalization (BN) and the ESN model introduced previously.

In the feature extraction stage, considering the parameter increase that traditional 3×3 convolutions might cause, the module utilizes decomposed convolution, a combination of 1×3 and 3×1 convolutions. This allows the network to independently extract features from both the width and height directions while maintaining sensitivity to local features

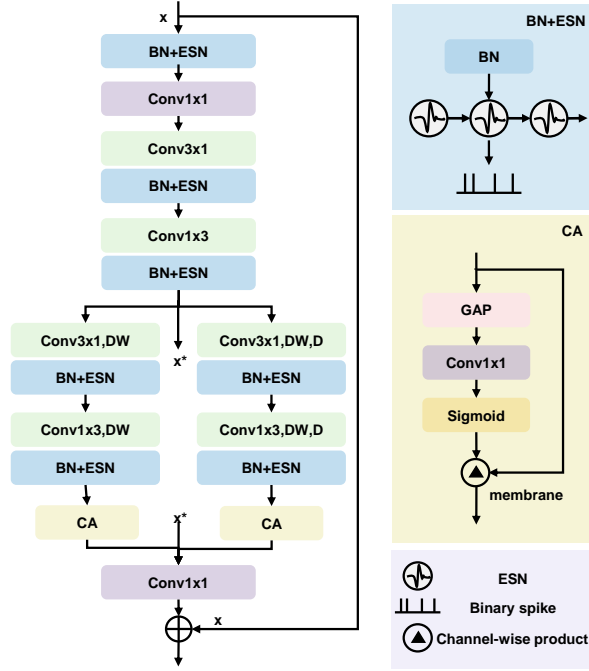


Fig. 2. The detailed construction of Spike-LD module. Among them, DW is depth-wise convolution, D denotes dilated convolution, GAP means global average pooling and *membrane* represents the membrane potential within the spiking neuron. ESN is an Evolutionary Spiking Neuron.

without increasing the parameters. Considering the importance of multi-scale features in event semantic segmentation tasks, our Spike-LD module introduces a three-branch structure, combining dilated and depth-wise convolution to capture features within different receptive fields. Moreover, to compensate for the loss of inter-channel interaction information caused by depth-wise convolution, the module employs channel attention (CA) modules [15] to improve the representation of features. Finally, 1×1 convolutions at the beginning and end of the module serve to compress and expand channel dimensions, respectively, to reduce the computational load of the model.

C. Spike-driven Transformer Block

Inspired by Yao et al. [16], we design a spike-driven transformer block (STB) as shown in the bottom of Fig. 3. It comprises a spike-driven multi-head self-attention module (SDMSA) aimed at capturing spatial relationships and a two-layer MLP complementing channel information. Specifically, the main process of STB is formulated as:

$$\begin{aligned} Q &= SN(\text{RepConv}_1(M)), \\ K &= SN(\text{RepConv}_2(M)), \\ V &= SN(\text{RepConv}_3(M)), \end{aligned} \quad (4)$$

$$\text{SDMSA}(Q, K, V) = \text{SUM}_c(Q \otimes K) \otimes V \quad (5)$$

$$\begin{aligned} M' &= M + \text{RepConv}_4(\text{SDMSA}(Q, K, V)), \\ \text{MLP}(M') &= \text{Linear}_2(\text{SN}_2(\text{Linear}_1(\text{SN}_1(M')))), \\ M'' &= M' + \text{MLP}(M'), \end{aligned} \quad (6)$$

where SN, RepConv, and \otimes are spiking neurons, re-parameterization convolution [17], and Hadamard product, respectively. We omit the BN operation for clarity.

The design of residual connections in spike transformers is critical; unlike the vanilla shortcut [18] and the spike-element-wise shortcut [19], we use the membrane shortcut, which performs shortcuts between membrane potentials to enhance performance while maintaining spiking features.

STB offers two key advantages over traditional CNN-transformer blocks. Firstly, as described in Eq. 5, the computational complexity is reduced to $O(N)$ instead of $O(N^2)$. Secondly, due to the use of spiking neurons, floating-point matrix multiplications are transformed into masked operations. This means that the entire block only involves floating-point addition operations, significantly reducing energy consumption and enhancing the computation efficiency.

III. OVERALL ARCHITECTURE OF SLTNET

To reduce computational load while maintaining semantic information from events, we design a Spike-driven Lightweight Transformer-based Network, called SLTNet, for event-based semantic segmentation based on the tailored efficient Spike-LD modules and STBs.

A. Event Representation

We encode the raw asynchronous event stream $e_i = \{(x_i, y_i, t_i, p_i)\}_{i \in \Delta t}$ into voxel grid $V_{k,x,y} \in K \times H \times W$:

$$V_{k,x,y} = \sum_{i \in \Delta t} \delta(\lfloor \frac{t_i}{\Delta t} \rfloor = k) \delta(x_i = x) \delta(y_i = y) p_i, \quad (7)$$

where Δt is time interval, time index $k = \lfloor \frac{t_i}{\Delta t} \rfloor$, δ denotes Kronecker Delta function used for indicating whether event e_i is within time period k and located at (x, y) , $p_i \in \{-1, +1\}$ represents the polarity. Furthermore, to adapt the spiking paradigm, we transform the voxel grid $V_{k,x,y}$ into an event tensor, formatted as $E(x, y, t) \in T \times K \times H \times H$ that SNNs could calculate through the temporal dimension. $E(x, y, t)$ will be fed into our SLTNet as event representations.

B. Spike-driven Encoder/Decoder of SLTNet

As shown in the top of Fig. 3, the preprocessed events $E(x, y, t)$ will pass through a hierarchical spiking encoder, a lightweight spiking decoder, and two segmentation head, generating two prediction probabilities maps, P_1 and P_2 .

The hierarchical spiking encoder starts with an initial block, which stacks three spike convolution layers, each consisting of a 3×3 vanilla convolution, batch normalization, and an ESN. Then, it goes through four stages: the first three stages are spike-driven convolution blocks (SCBs), each consisting of a downsampling layer and three spike-LD modules with different dilation rates, and the last stage includes two STBs. The SCB can extract local detail information, while the STB enriches the long-range context information that complements the local features. The downsampling layers applied in stages 1 to 3 consist of stridden convolutions and pooling operations, transforming the feature dimensions from $C \times H \times W$ to $8C \times \frac{H}{8} \times \frac{W}{8}$. However, to reduce the

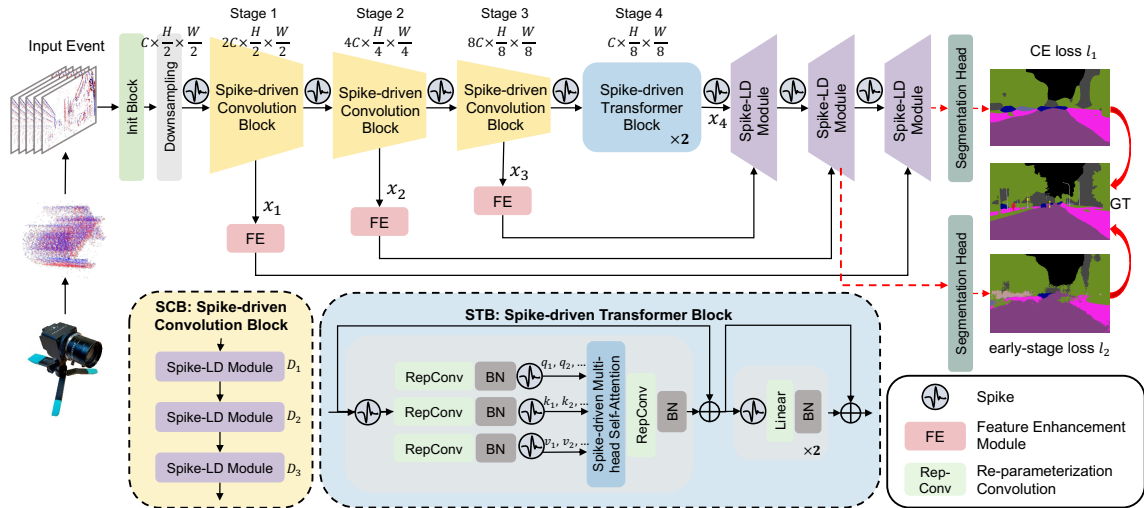


Fig. 3. The architecture of SLTNet, where input events are passed through a four-stage spiking encoder built on SCBs and STBs. Then, features are enhanced by three Spike-LD modules in the decoder. Finally, two separate segmentation heads generate two prediction probability maps at different levels.

computational cost, we narrow the feature channels to C before feeding into the STB. In addition, we place ESN between blocks to ensure spike transmission.

The lightweight spiking decoder is composed of three upsampling stages, each containing a Spike-LD module, an upsampling layer implemented using transposed convolution, BN, and final pass through ESN neurons. To restore the spatial detail encoded in the earlier stage, we sequentially add the feature map generated by stages 1, 2, and 3 to different levels of decoders. Before fusion, the extracted event features x_1 , x_2 , and x_3 are enhanced by the feature enhancement (FE) module [20]. Finally, output features F_1 and F_2 are passed into two segmentation heads, generating two prediction probabilities maps, i.e., P_1 and P_2 .

C. Segmentation Loss Design

As illustrated in Fig. 3, the designed loss consists of a cross-entropy (CE) semantic loss l_1 using Online Hard Example Mining (OHEM) [21] and an early-stage CE semantic loss l_2 . Specifically, we use l_1 equipped with OHEM to improve the generalization ability by selecting the hardest samples from each mini-batch for training:

$$l_1 = \sum_{i \in S} (-\sum_{j=1}^C y_j^i \log(\hat{y}_j^i)), \quad l_2 = \sum_i (-\sum_{j=1}^C y_j^i \log(\hat{y}_j^{\text{early},i})), \quad (8)$$

where S is the set containing the top k percent of the largest losses among l_i . l_2 is employed to promote rapid convergence. It measures the discrepancy between the predicted probabilities, which are generated from the second-to-last Spike-LD module, and ground-truth label.

Therefore, the entire loss in our SLTNet is: $Loss = \lambda_1 l_1 + \lambda_2 l_2$. In our experiments, $\lambda_1=1.0$, $\lambda_2=0.4$, $k=0.7$.

IV. EXPERIMENTS AND RESULTS

A. Experimental Datasets

We validate our method on two public large-scale event-based automotive driving datasets: the commonly used

DDD17 benchmark [22] and the DSEC-Semantic dataset [23] with higher quality semantic labels and colored images. They both include diverse driving scenarios and weather conditions. Following the previous settings, we evaluate our method on the officially released test set.

B. Implementation Details

Experiments are conducted on a single Nvidia GTX4090 GPU with 24 GB of memory. We train our model using Adam Optimizer with StepLR strategy. Training epochs, initial learning rate, weight decay, batch size, step size, and γ in the StepLR strategy for DDD17 and DSEC-Semantic datasets are [300, 1e-3, 1e-4, 64, 5, 0.92] and [500, 1e-3, 1e-4, 16, 10, 0.92], respectively. For the LIF neuron in the ESN model, we set the reset value $U_{reset} = 0$, the membrane time constant $\tau = 0.25$, and the spike firing threshold $U_{th} = 1.0$. In the event representation, the time interval $\Delta t = 50$ ms and the membrane time constant $T = 1$.

C. Comparison with State-of-the-art Methods

Given the limited number of studies on event-based semantic segmentation, our primary comparison involves several well-known methods, spanning two kinds of neural networks: ANNs and SNNs. For ANNs, we evaluate our approach against Ev-SegNet [7], Evdistill [9], and ESS [10]. In SNNs, we reimplemented Spiking-DeepLab and Spiking-FCN according to the network structure and implementation details described in [12]. Due to unavailable code, we are unable to evaluate EvDistill on the DSEC-Semantic Dataset.

1) *Performance on DDD17*: Detailed results are given in Tab. I. In the field of SNNs, our SLTNet achieves the highest segmentation performance while maintaining the smallest number of parameters, minimal floating-point computations, and the fastest inference speed. Specifically, we achieve 7.30% and 9.06% higher mIoU than Spiking-DeepLab and Spiking-FCN, respectively. Meanwhile, it has $38.76\times$ fewer

TABLE I
SEGMENTATION COMPARISON OF DIFFERENT ANN/SNN MODELS ON DDD17 AND DSEC-SEMANTIC DATASET.

Dataset	Model	Data	Type	Params. (M) ↓	FLOPs (G) ↓	FPS ↑	mIoU (%) ↑
DDD17	Ev-SegNet	Event	ANN	23.75	44.17	20.67	54.81
	Evdistill	Event+Frame	ANN	58.64	65.08	2.96	58.02
	ESS	Event+Frame	ANN	6.69	-	-	61.37
	Spiking-DeepLab	Event	SNN	15.89	4.05	100	44.63
	Spiking-FCN	Event	SNN	18.64	35.23	72.73	42.87
	SLTNet (Ours)	Event	SNN	0.41	1.96	114.29	51.93
DSEC-Semantic	Ev-SegNet	Event	ANN	23.75	-	-	51.76
	ESS	Event+Frame	ANN	6.69	-	-	51.57
	Spiking-DeepLab	Event	SNN	15.89	14.02	100	44.58
	Spiking-FCN	Event	SNN	18.64	126.46	17.78	38.52
	SLTNet (Ours)	Event	SNN	1.67	6.97	114.29	47.91

TABLE II
ENERGY CONSUMPTION OF DIFFERENT ANN/SNN MODELS ON DDD17 DATASET.

Model	Type	MAC	ACC	Energy (mJ) ↓
Ev-SegNet	ANN	9322 M	0 M	42.88 (30.20×)
Evdistill	ANN	29730 M	0 M	136.76 (96.31×)
ESS	ANN	11700 M	0 M	53.82 (37.90×)
Spiking-DeepLab	SNN	1435 M	2617 M	7.78 (5.48×)
Spiking-FCN	SNN	264 M	35176 M	17.04 (12.00×)
SLTNet (Ours)	SNN	131 M	1830 M	1.42 (1.00 ×)

parameters, $2.07\times$ less GFLOPs, and $1.14\times$ faster FPS than comparative SNN methods.

Next, we compare SLTNet to other ANN methods. Though our SLTNet slightly lags behind Ev-SegNet, it requires $57.93\times$ fewer parameters, $22.54\times$ less FLOPs, and achieves $5.53\times$ faster FPS. Although there is a performance gap in mIoU compared to Evdistill and ESS, SLTNet achieves these results without using any image information and with significantly lower energy consumption and parameters. The energy consumption will be discussed in detail later. We present qualitative results in Fig. 4 to provide a more intuitive comparison of different models. Our proposed method achieves fine-grained segmentation compared to competition models, which demonstrates the effectiveness of our design.

2) *Performance on DSEC-Semantic*: As shown in Table. I, our model achieves the best segmentation result within the SNN field, with a performance of 47.91% mIoU. Specifically, it outperforms Spiking-DeepLab by 3.33% with $9.51\times$ fewer parameters and Spiking-FCN by 9.39% with $11.16\times$ fewer parameters. Though our model still falls behind ANN-based methods, the gap between them has significantly narrowed compared to the DDD17 dataset as the spatial resolution of the event data increases. At the same time, SLTNet achieves fewer parameters (1.67 M) and FLOPs (6.97 G) across all ANN and SNN methods, which demonstrates superior performance in computation efficiency and process speed, achieves promising 114.29 FPS.

TABLE III
ABLATION STUDIES OF SPIKE-DRIVEN MULTI-HEAD SELF-ATTENTION METHOD ON DDD17.

Self-attention	mIoU (%)
SDSA2 [24]	50.77 (-1.16)
SDSA3 [24]	51.00 (-0.93)
Spike-driven Transformer [25]	49.70 (-2.23)
Spikformer [26]	48.74 (-3.19)
SDMSA (Ours)	51.93

D. Power and Computation Cost Analysis

Floating-point operations (FLOPs) are widely recognized for evaluating the computational load of neural networks. In ANNs, FLOPs almost come from floating-point matrix multiplication and accumulation (MAC). Since the event-driven characteristics of SNNs, the binary spikes transmitted within them result in almost all FLOPs being accumulation (ACC). Combining the timestep $T = 1$ and spiking firing rate $R = 0.5$, we can estimate the energy consumption of SNNs:

$$E = E_{MAC} \times FL_1 + E_{ACC} \times FL_2 \times T \times R. \quad (9)$$

where FL can be FLOPs of the convolution or linear layer.

Table II compares energy consumption with other models. To maintain consistency with previous work [12], we set $E_{MAC} = 4.6pJ$ and $E_{AC} = 0.9pJ$ during calculation. Compared to ANN-based models, our proposed SLTNet excels in energy efficiency. Specifically, Ev-SegNet, Evdistill, and ESS consume $30.20\times$, $96.31\times$, and $37.90\times$ more energy than our model, respectively. Although Spiking-DeepLab and Spiking-FCN also utilize spiking architectures, their straightforward components and design result in $5.48\times$ and $12.00\times$ higher power consumption.

E. Ablation Studies

1) *Spike-driven Multi-head Self-attention*: In SNNs, the query, key, and value in self-attention are represented as binary spikes rather than continuous floating-point values. Therefore, traditional self-attention modules designed for ANNs are not directly applicable to SNNs. Developing an efficient self-attention mechanism specifically optimized for SNNs remains a challenge. In Table III, we present

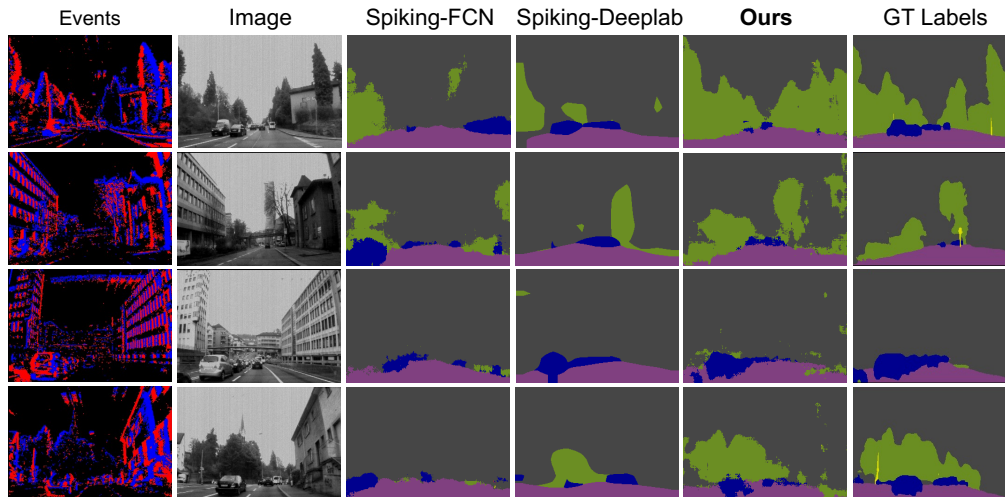


Fig. 4. Qualitative segmentation results on the DDD17 dataset. The left is event frame and its corresponding image frame. The rightmost is ground truth.

TABLE IV
ABLATION STUDIES OF SLTNET ON DDD17.

Ablation	Module	Params. (M)	mIoU (%)
Shortcut	MS \rightarrow VS	0.41	49.03 (-2.90)
	MS \rightarrow SEW	0.41	32.55 (-19.38)
Architecture	SLTNet w/o FE	0.41	49.97 (-1.96)
	SLTNet w/o STB	0.41	48.47 (-3.46)
	SLTNet w/o Fusion	0.41	49.66 (-2.27)
Ours	SLTNet	0.41	51.93

a performance comparison between our SDMSA attention module and other spike-driven attention/transformer modules, described in Eq. 5. The results show that our proposed SDMSA outperforms other methods by at least 1.16% mIoU when evaluated by the same model. Besides, the proposed SDMSA module is 2.23% and 3.19% higher than the recently proposed spike-driven transformer [25] and Spikformer [26].

2) *Shortcut and Architecture*: The ablation parts on the network architecture have almost no impact on the number of parameters, effectively eliminating the effect of parameter space on performance. **Shortcut**. There are three shortcuts in SNNs, where we use the membrane shortcut (MS) that connects float membrane potential in different layers. The other two are the Spike-Element-Wise (SEW) [19] Shortcut, which fuses spikes across layers, and the Vanilla Shortcut (VS) [18], which directly connects spikes to membrane potential. As shown in Table IV, in our architecture, our MS performs the best, with VS reducing the segmentation accuracy by 2.90% and SEW shortcut by 19.38%. The poor performance of SEW shortcut indicates that using spikes alone without retaining information about the membrane potential can significantly impair performance on tasks requiring detailed information. **Architecture**. When removing the FE module in the skip connection, the mIoU is reduced by 1.96%, demonstrating its effectiveness in enhancing feature expression. Furthermore, we change the network to fully SCBs without STBs. Performance dropped by 3.46%

TABLE V
ABLATION STUDIES OF LOSS DESIGN.

OHEM Loss (l_1)	Early Loss (l_2)	mIoU (%)
×	×	47.43 (-4.50)
×	✓	48.46 (-3.47)
✓	×	49.63 (-2.30)
✓	✓	51.93 (Ours)

significantly, which proves that transformer and convolution blocks can achieve complementarity. Then, we remove the skip connection from stages 1-3 as described in Sec. III-B. It leads to a performance loss of 2.27%, showing that the feature map from the early stage can effectively complement segmentation information.

3) *Loss Design*: To verify the effectiveness of our loss design, we conduct four groups of ablation experiments on different combinations of two losses in Table V. The results show that using conventional cross-entropy loss (no OHEM and Early loss) leads to a huge performance drop, especially a 4.50% decrease in mIoU. Notably, the optimization effect of OHEM loss becomes apparent with the help of Early loss, which is 3.47% and 2.30% higher than employing OHEM loss alone and early loss alone, respectively.

V. CONCLUSIONS

In this work, we tackle the real-world challenges of traditional semantic segmentation by designing lightweight single-branch architecture and integrating them into the spike-based paradigm. We design a spike-driven lightweight transformer-based network, named SLTNet, that is built on efficient SCBs and STBs basic blocks. Extensive experimental results show that our work outperforms SOTA SNN-based methods on both DDD17 and DSEC-Semantic datasets. SLTNet also achieves $2.01\times$ more computational load saving, $5.48\times$ more energy-saving, and $1.14\times$ faster inference speed. In the future, we will extend our method to other fields, such as simultaneous localization mapping, and flow estimation.

REFERENCES

- [1] A. Garcia-Garcia, S. Orts-Escolano, S. Oprea, V. Villena-Martinez, and J. Garcia-Rodriguez, "A review on deep learning techniques applied to semantic segmentation," *arXiv preprint arXiv:1704.06857*, 2017.
- [2] X. Long, H. Zhao, C. Chen, F. Gu, and Q. Gu, "A novel wide-area multiobject detection system with high-probability region searching," in *2024 IEEE International Conference on Robotics and Automation (ICRA)*, 2024, pp. 18 316–18 322.
- [3] H. Zhao, J. Shang, K. Liu, C. Chen, and F. Gu, "Edgevo: An efficient and accurate edge-based visual odometry," in *2023 IEEE International Conference on Robotics and Automation (ICRA)*, 2023, pp. 10 630–10 636.
- [4] A. Abdullah, T. Barua, R. Tibbetts, Z. Chen, M. J. Islam, and I. M. Rekleitis, "Caveseg: Deep semantic segmentation and scene parsing for autonomous underwater cave exploration," in *2024 IEEE International Conference on Robotics and Automation (ICRA)*, 2023, pp. 3781–3788.
- [5] J. Cao, X. Zheng, Y. Lyu, J. Wang, R. Xu, and L. Wang, "Chasing day and night: Towards robust and efficient all-day object detection guided by an event camera," in *2024 IEEE International Conference on Robotics and Automation (ICRA)*, 2024, pp. 9026–9032.
- [6] G. Gallego, T. Delbrück, G. Orchard, C. Bartolozzi, B. Taba, A. Censi, S. Leutenegger, A. J. Davison, J. Conradt, K. Daniilidis *et al.*, "Event-based vision: A survey," *IEEE transactions on pattern analysis and machine intelligence*, vol. 44, no. 1, pp. 154–180, 2020.
- [7] I. Alonso and A. C. Murillo, "Ev-segnet: Semantic segmentation for event-based cameras," in *Proceedings of the IEEE/CVF Conference on Computer Vision and Pattern Recognition Workshops*, 2019, pp. 0–0.
- [8] L. Wang, Y. Chae, and K.-J. Yoon, "Dual transfer learning for event-based end-task prediction via pluggable event to image translation," in *Proceedings of the IEEE/CVF International Conference on Computer Vision*, 2021, pp. 2135–2145.
- [9] L. Wang, Y. Chae, S.-H. Yoon, T.-K. Kim, and K.-J. Yoon, "Evdistill: Asynchronous events to end-task learning via bidirectional reconstruction-guided cross-modal knowledge distillation," in *Proceedings of the IEEE/CVF Conference on Computer Vision and Pattern Recognition*, 2021, pp. 608–619.
- [10] Z. Sun, N. Messikommer, D. Gehrig, and D. Scaramuzza, "Ess: Learning event-based semantic segmentation from still images," in *European Conference on Computer Vision*. Springer, 2022, pp. 341–357.
- [11] S. Ghosh-Dastidar and H. Adeli, "Spiking neural networks," *International journal of neural systems*, vol. 19, no. 04, pp. 295–308, 2009.
- [12] Y. Kim, J. Chough, and P. Panda, "Beyond classification: Directly training spiking neural networks for semantic segmentation," *Neuromorphic Computing and Engineering*, vol. 2, no. 4, p. 044015, 2022.
- [13] Y. Guo, Y. Chen, L. Zhang, X. Liu, Y. Wang, X. Huang, and Z. Ma, "Im-loss: information maximization loss for spiking neural networks," *Advances in Neural Information Processing Systems*, vol. 35, pp. 156–166, 2022.
- [14] K. He, X. Zhang, S. Ren, and J. Sun, "Deep residual learning for image recognition," *2016 IEEE Conference on Computer Vision and Pattern Recognition (CVPR)*, pp. 770–778, 2015. [Online]. Available: <https://api.semanticscholar.org/CorpusID:206594692>
- [15] J. Hu, L. Shen, and G. Sun, "Squeeze-and-excitation networks," in *2018 IEEE/CVF Conference on Computer Vision and Pattern Recognition*, 2018, pp. 7132–7141.
- [16] M. Yao, J. Hu, T. Hu, Y. Xu, Z. Zhou, Y. Tian, B. XU, and G. Li, "Spike-driven transformer v2: Meta spiking neural network architecture inspiring the design of next-generation neuromorphic chips," in *The Twelfth International Conference on Learning Representations*, 2024. [Online]. Available: <https://openreview.net/forum?id=1SIBN5Xyw7>
- [17] S. Deng and S. Gu, "Optimal conversion of conventional artificial neural networks to spiking neural networks," in *International Conference on Learning Representations*, 2021. [Online]. Available: <https://openreview.net/forum?id=FZ1oTwcXchK>
- [18] K. He, X. Zhang, S. Ren, and J. Sun, "Deep residual learning for image recognition," in *Proceedings of the IEEE conference on computer vision and pattern recognition*, 2016, pp. 770–778.
- [19] W. Fang, Z. Yu, Y. Chen, T. Huang, T. Masquelier, and Y. Tian, "Deep residual learning in spiking neural networks," *Advances in Neural Information Processing Systems*, vol. 34, pp. 21 056–21 069, 2021.
- [20] G. Xu, J. Li, G. Gao, H. Lu, J. Yang, and D. Yue, "Lightweight real-time semantic segmentation network with efficient transformer and cnn," *IEEE Transactions on Intelligent Transportation Systems*, vol. 24, no. 12, pp. 15 897–15 906, 2023.
- [21] A. Shrivastava, A. Gupta, and R. Girshick, "Training region-based object detectors with online hard example mining," in *2016 IEEE Conference on Computer Vision and Pattern Recognition (CVPR)*, 2016, pp. 761–769.
- [22] J. Binas, D. Neil, S.-C. Liu, and T. Delbruck, "Ddd17: End-to-end davis driving dataset," *arXiv preprint arXiv:1711.01458*, 2017.
- [23] Z. Sun, N. Messikommer, D. Gehrig, and D. Scaramuzza, "Ess: Learning event-based semantic segmentation from still images," in *European Conference on Computer Vision*. Springer, 2022, pp. 341–357.
- [24] M. Yao, J. Hu, T. Hu, Y. Xu, Z. Zhou, Y. Tian, B. XU, and G. Li, "Spike-driven transformer v2: Meta spiking neural network architecture inspiring the design of next-generation neuromorphic chips," in *The Twelfth International Conference on Learning Representations*, 2024. [Online]. Available: <https://openreview.net/forum?id=1SIBN5Xyw7>
- [25] M. Yao, J. Hu, Z. Zhou, L. Yuan, Y. Tian, B. XU, and G. Li, "Spike-driven transformer," in *Thirty-seventh Conference on Neural Information Processing Systems*, 2023. [Online]. Available: <https://openreview.net/forum?id=9FmolyOHi5>
- [26] Z. Zhou, Y. Zhu, C. He, Y. Wang, S. YAN, Y. Tian, and L. Yuan, "Spikformer: When spiking neural network meets transformer," in *The Eleventh International Conference on Learning Representations*, 2023. [Online]. Available: https://openreview.net/forum?id=frE4fUwz_h